Solvent evaporation and interdiffusion in polymer films

2005 J. Phys.: Condens. Matter 17 S4119

(http://iopscience.iop.org/0953-8984/17/49/008)

INSTITUTE OF PHYSICS PUBLISHING JOURNAL OF PHYSICS: CONDENSED MATTER

J. Phys.: Condens. Matter **17** (2005) S4119–S4132 doi:10.1088/0953-8984/17/49/008

Solvent evaporation and interdiffusion in polymer films

Mesfin Tsige and Gary S Grest

Sandia National Laboratories, Albuquerque, NM 87185, USA

E-mail: mtsige@sandia.gov and gsgrest@sandia.gov

Received 18 July 2005, in final form 9 September 2005
Published 25 November 2005
Online at stacks.iop.org/JPhysCM/17/S4119

Abstract

Solvent evaporation from homopolymer and heteropolymer films along with the interdiffusion of solvent into these films are studied by molecular dynamics simulations. Due to the high viscosity of polymer melts, in many cases polymer films are made by first dissolving the polymer in a low viscosity solvent, spreading the solution on a substrate and subsequently evaporating the solvent. Here we study the last part of this process, namely the evaporation of solvent from a polymer film. As the solvent evaporates, the polymer density at the film/vapour interface is found to increase sharply, creating a polymer density gradient which acts as a barrier for further solvent evaporation. For both homopolymer and heteropolymer films, the rate of solvent evaporation is found to decrease exponentially as a function of time. For multiblock copolymer films the resulting domain structure is found to be strongly affected by the relative stiffness of the two blocks. The reverse process, namely the interdiffusion of solvent into a polymer film, is also studied. For homopolymer films the weight gain by the film scales as $t^{1/2}$, which is expected for Fickian diffusion. The diffusivity $D(c)$ determined from the one-dimensional Fick's diffusion equation agrees well with that calculated from the corrected diffusion constant using the Darken equation. Far above the polymer glass transition temperature, $D(c)$ is nearly independent of concentration. However, as the temperature decreases $D(c)$ is found to depend strongly on the state of the polymer and is related to the shape of the solvent concentration profile. Finally, the swelling of a multiblock copolymer film in which the stiffer block is below its glass transition temperature is also studied. While the solvent swells only the softer block of the copolymer, the weight gain by the film remains Fickian.

(Some figures in this article are in colour only in the electronic version)

1. Introduction

Many practical applications and modern technologies rely on the diffusion of small molecule penetrants within or through a polymeric film or membrane. Applications include controlled drug release, food storage, and membrane separations [1–6]. In general, the transport properties of penetrants through a polymeric matrix are determined by the chemical and physical properties of both the polymer and the penetrant. The interdiffusion of penetrants into a polymer depends on the penetrant concentration gradient within the system as well as the rate of polymer segmental relaxation. Well above the polymer glass transition the diffusion is usually well described as Fickian or case I, in which case the mass uptake of the penetrant solvent or the distance covered by the solvent as a function of time increases as $t^{1/2}$. Non-Fickian kinetics are expected when the viscoelastic properties of the polymer become the determining factor. This case is often referred to as case II diffusion and the mass uptake of solvent is linearly increasing with time.

The interdiffusion of a solvent film placed in contact with one surface of a homopolymer melt film can often be described by the one-dimensional diffusion equation [7]

$$\frac{\partial c}{\partial t} = \frac{\partial}{\partial z}\left(D(c)\frac{\partial c}{\partial z}\right), \tag{1}$$

where c is the solvent concentration in units of mass per unit volume and $D(c)$ is the diffusivity. This equation assumes that the volume of the medium is not changed by the interdiffusion of the solvent. $D(c)$ is in general dependent on c and except in special cases such as $D(c) = D_0$ is independent of solvent concentration; equation (1) has to be solved numerically [7]. For constant $D(c)$, equation (1) can be solved analytically and the concentration of solvent in the medium as a function of position and time is

$$c(z, t) = c_0(1 - \mathrm{erf}(z/2\sqrt{(D_0 t)})). \tag{2}$$

where c_0 is the equilibrium solvent concentration in the polymer and erf is the error function. This simple functional form of equation (2) is often used to fit experimental data even if the solvent swells the polymer and $D(c)$ may not be independent of c [7]. It is important to note that in general the diffusivity $D(c)$ is not equal to the self- or tracer diffusion constant $D_s(c)$ of the solvent. Only in the limit of low concentration, as discussed below, is $D(c) = D_s(c)$.

If the diffusivity $D(c)$ is only a function of c, a Boltzmann transformation of equation (1) gives

$$\frac{\partial z}{\partial t} = f(D, c)t^{1/2} \tag{3}$$

where $f(D, c)$ is a function of D and c only. This equation, regardless of the functional form of $D(c)$, reflects the square root time dependence that is a fingerprint of Fickian diffusion.

Transport properties of a solvent into a heteropolymer can be more complex [8–11]. For example, copolymers are known to self-assemble into a microdomain structure, which can impose spatial constraints on a diffusing solvent and can lead to anisotropic behaviour. How this microdomain structure changes in solution is a topic of current interest, mainly due to its potential application for nanotechnology. The morphology of the polymer film can be influenced by a number of factors, such as polymer chain length and its chemical structure, block length, temperature, and thermodynamic compatibility of the solvent with the components of the copolymer. For a given copolymer system, a neutral solvent is expected to distribute itself equally between the two microdomains while a slight difference in solvent selectivity between the block of the copolymer can lead to an observable preferential swelling of one component [12, 13]. Very little is known about the affinity of a solvent in a copolymer

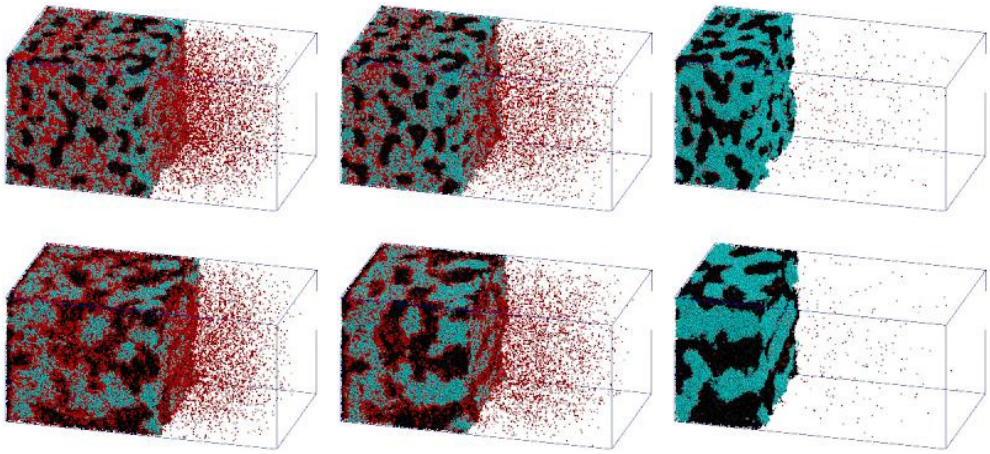

Figure 1. Snapshots of the evaporation process for system II (upper panels) and IV (lower panels), listed in table 1, at 25%, 50%, and 94% evaporated solvent. Solvent monomers are coloured red, and type 2 and type 3 polymer monomers are coloured green and black, respectively. Note that the ordering appears as a result of solvent evaporation. The direction of evaporation is $\hat{z}$ and is perpendicular to both $\hat{x}$ and $\hat{y}$.

with variable stiffness between the block segments. We have recently shown [14] that varying only the stiffness of the block segments of the copolymer can result in rich microdomain structures as shown in figure 1. As far as we are aware, no systematic study has been carried out to examine the distribution of solvent in copolymers with variable block stiffness, though the single-chain behaviour in selective solvent has recently been reported [15, 16].

Molecular dynamics (MD) simulations have become a powerful tool for studying polymeric systems. For homopolymers, a variety of methods [17] have now been developed to generate well equilibrated melt configurations which can be used to start a simulation. The same is not the case for all but the simplest heteropolymers. For example, for a diblock copolymer system, if the ordered phase is lamellar, then it is straightforward to generate starting states [18] with the correct lamellar spacing. However, if the ordered phase is spherical or cylindrical, there is at present no method which can create an initial starting state with the correct lattice spacing and domain size. The problem is that the structure of the equilibrated heteropolymer film is not generally known *a priori*. Even if known, as in the case of a diblock copolymer, generating an equilibrated starting configuration is at present an unsolved problem. One way of computationally producing polymer films is to follow the experimental procedure of dissolving the polymer in a solvent and then evaporating the solvent. We followed this procedure, as shown in figure 1, to generate the initial configuration for studying computationally the interdiffusion of solvent into heteropolymer films [14]. For comparison we also studied the evaporation from a homopolymer film [19], which somewhat surprisingly has not been well studied experimentally.

The paper is organized as follows. In the following section we briefly discuss the model and the force field used to describe our systems. Simulation details about the system set-up and size are also discussed. In section 3 the results for the evaporation study of solvent from both homo- and heteropolymers are presented. Special attention is given to how the evaporation process affects the structure of the film. For the heteropolymer case, emphasis is also given on how differences in block length affect the final morphology of the system. In section 4 the interdiffusion results for both homo- and heteropolymers are presented. For the homopolymer

case, the relation between various diffusion coefficients is discussed. The main results are summarized in section 5.

2. Model and simulation details

2.1. Model

To represent the polymer chains we used the coarse grained bead–spring model in which the bead size defines the excluded-volume interactions while the springs describe chain connectivity. The homopolymer system is represented by freely jointed bead–spring chains of length N monomers of mass m, while the block copolymer systems are represented by bead–spring chains of different block and chain lengths consisting of two different species each of the same mass m. In all cases, the solvent is modelled as single monomers of mass m. We denote the solvent monomers as type 1 and the two species of the polymer as types 2 and 3, which corresponds to the softer and stiffer part of the copolymer, respectively.

Nonbonded pairs of monomers of type α and β interact through the standard 6–12 Lennard-Jones potential

$$U_{\mathrm{LJ}}(r) = \begin{cases} 4\epsilon_{\alpha\beta}\left\{\left(\frac{\sigma_{\alpha\beta}}{r}\right)^{12} - \left(\frac{\sigma_{\alpha\beta}}{r}\right)^{6}\right\} + \epsilon_{\mathrm{LJ}}, & r \leqslant r_{\mathrm{c}} \\ 0, & r > r_{\mathrm{c}} \end{cases} \tag{4}$$

where r is the distance between monomers and ϵ_{LJ} is a constant added so that the potential is continuous at $r = r_{\mathrm{c}}$. Here we take the effective excluded-volume diameter of the beads $\sigma_{\alpha\beta} = \sigma$ for all α, β, and the cut-off radius $r_{\mathrm{c}} = 2.5\sigma$ except between the two different species of the copolymer, where the interaction is purely repulsive, $r_{\mathrm{c}} = 2^{1/6}\sigma$. The depth of the attractive minimum is set to $\epsilon_{\alpha\beta} = \epsilon$ for all α and β except in the interdiffusion study of copolymers, where $\epsilon_{33} = 2\epsilon$ is used in order for the stiff blocks to be below their glass transition temperature.

In addition to the Lennard-Jones interaction between bonded monomers we add an anharmonic interaction term known as the FENE potential [20, 21],

$$U(r) = \begin{cases} -0.5R_0^2 k \ln[1 - (r/R_0)^2], & r \leqslant R_0 \\ \infty, & r < R_0 \end{cases} \tag{5}$$

where, as in previous studies [20, 21], $R_0 = 1.5\sigma$ and $k = 30\epsilon$.

For the block copolymer systems a bending potential is imposed between the three neighbouring beads along the same chain [17]

$$U_{\mathrm{bend}}(\theta) = k_{\theta,\alpha}(1 - \cos\theta) \tag{6}$$

where $k_{\theta,\alpha}$ is the elasticity parameter and depends on the type of the central monomer and θ is the angle formed between two adjacent bonds. The stiffness parameters used in most of the present studies are $k_{\theta,1} = 3$ for type 2 and $k_{\theta,2} = 10$ for type 3.

All the simulations were run at a temperature of $T = \epsilon/k_{\mathrm{B}}$, where k_{B} is the Boltzmann constant. For the homopolymer the glass transition temperature for the model is $T_{\mathrm{g}} = 0.5$–$0.6\epsilon/k_{\mathrm{B}}$ [22]. The equations of motion were integrated with a velocity Verlet algorithm with a time step of $\Delta t = 0.01\tau$ for the evaporation and interdiffusion study and $\Delta t = 0.009\tau$ for the bulk equilibrium measurement of the self- and corrected diffusion constants in a homopolymer melt. Here $\tau = \sigma(m/\epsilon)^{1/2}$ is the standard LJ unit of time.

Table 1. Parameter for the four multiblock systems studied. Range of block length, number of blocks per chain, and polydispersity index P.

System	Block length	Number of blocks	P
I	10	10	1.0
II	10–20	5–20	1.14
III	30–60	3–12	1.16
IV	20–100	2–20	1.27

2.2. *Simulation details*

2.2.1. Evaporation. For both homopolymer and block copolymer systems studied the initial configuration is created by randomly building the polymer chains between two flat walls where beads are initially allowed to overlap and then the overlap removed by applying a soft nonbonded potential. The system is then equilibrated at pressure $P \simeq 0$ and temperature $T = \epsilon/k_B$, by allowing the distance between the two walls to adjust. The monomer–surface interaction potential is given by the 9–3 LJ potential with a cut-off distance of $r_c^w = 2.2\sigma$ [23]. The surface interaction is chosen to be strong enough that a vapour phase [24] does not form between the polymer and the wall. After equilibration, the top wall is then removed so that the solution is in contact with a vacuum. Periodic boundary conditions are used in the x- and y-directions, and the solvent evaporates in the z-direction. The evaporated solvent monomers are removed from the system when they reach a specified distance far above the original film. This is done by using the massively parallel grand canonical MD code LADERA [25], which is a hybrid of the massively parallel MD code LAMMPS [26] and a grand canonical Monte Carlo (GCMC) code [27].

The initial configuration of the homopolymer system consists of 600 polymer chains of length $N = 500$ monomers dissolved in 300 000 solvent monomers with $L_x = L_y = 100\sigma$. For the case of multi-block copolymers, four systems, listed in table 1, with $L_x = L_y = 80\sigma$ were studied. The systems differ in the number and length of the blocks, though in each case the stiffness of the two blocks remains unchanged, namely $k_{\theta,2} = 3$ and $k_{\theta,3} = 10$, except for system I, where either $k_{\theta,2} = 1$ or 3 is used. The fraction of each component is equal for all four cases. Additional results for different stiffnesses of the two blocks for the ordered case (system I) can be found in [14]. System I is ordered with each block having ten monomers per block and ten blocks per chain. For the remaining three systems, the block length and number of blocks per chain are chosen randomly from the values listed in the table. The polydispersity index P, measured as the ratio of number- and weight-average degrees of polymerization of the chains, is also listed in table 1 and ranges from 1.0 to 1.27. While the range of block length in each case is small compared to experiment, some differences in these cases can be identified as discussed in section 3. For case I, the total number of polymer monomers is $N_p \simeq 200\,000$, dissolved initially in an equal number of solvent monomers N_s. For the remaining three cases, the total number of polymer monomers $N_p \simeq 250\,000$, dissolved in $N_s \simeq 250\,000$ solvent monomers. Each system is allowed to equilibrate for $\simeq 10^5\tau$ before solvent is allowed to evaporate.

2.2.2. Interdiffusion. For the interdiffusion of solvent monomers into a polymer melt, the simulated system consists of a polymer melt in contact with solvent monomers only on one side of the rectangular box [28, 29]. For the homopolymer melt case, the polymer melt was first equilibrated between two walls at pressure $P \simeq 0$ and then the top of the box was extended and a thick layer of solvent monomers placed in contact with the polymer. The homopolymer melt

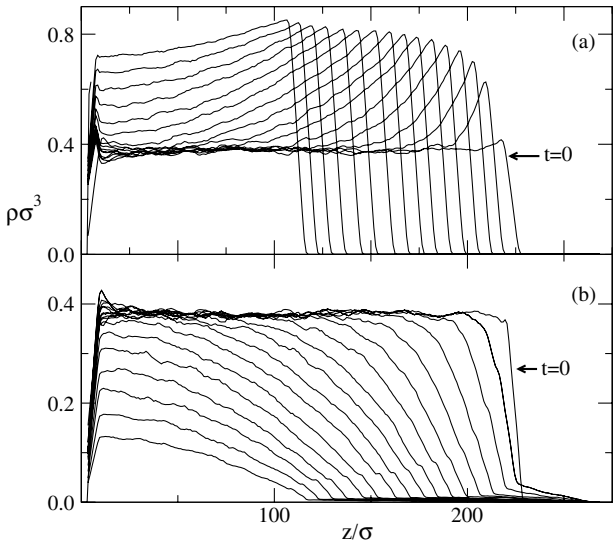

Figure 2. Time evolution of the density profile in the solvent evaporation direction for (a) polymer and (b) solvent during the evaporation process in the homopolymer system. The profiles are at different times and from right to left correspond to $t/(10^3\tau) = 0$, 4, 10, 20, 30, 40, 60, 80, 100, 140, 180, 220, 260, 310, 360, 430. The substrate is at $z = 0$.

consisted of 600 chains of length $N = 500$ monomers. The number of solvent monomers was 230 000. For the multi-block copolymer case, the final state of the three random copolymers (systems II–IV) were used as starting states for the interdiffusion study. The only difference from the evaporation is that the interaction ϵ_{33} between the stiffer blocks was increased to $\epsilon_{33} = 2\epsilon$ so that the film would only swell a finite amount as is typically of many applications such as polymer membranes for fuel cells.

For the homopolymer case, separate simulations [29] of an equilibrated polymer solvent mixture in a cubic simulation cell with periodic boundary conditions in all directions were carried out to compare the diffusivity $D(c)$ obtained from the Darken equation with that measured from the interdiffusion study using the one-dimensional Fick's model. M chains of length $N = 500$ monomers, where $M = 100$ for solvent concentration $c < 0.45\sigma^{-3}$ and $M = 50$ for $c \geqslant 0.45\sigma^{-3}$, were used in these simulations. A pure solvent system of 50 000 monomers was also simulated.

3. Evaporation

A typical density profile of polymer and solvent as a function of time is presented in figure 2 for solvent evaporating from a homopolymer film. Two important features are observed in the evaporation process. First, the density of the polymer increases to its equilibrium melt density value ($\rho \simeq 0.8\sigma^{-3}$) by reducing the film thickness. Second, there is a sharp increase in polymer density at the film/vapour interface which results in a polymer density gradient across this interface. This is in agreement with the prediction of Bornside *et al* [30]. Using a one-dimensional model for the spin coating process they predicted that the region near the free surface becomes polymer rich first due to solvent evaporation. So far, this prediction has not been directly verified experimentally, though Richardson *et al* [31] have recently found a decrease in the rate of solvent evaporation from a spin cast PMMA thin film. This observation

can actually be related to the polymer density gradient as discussed below. de Gennes [32] also pointed out that for glassy polymers this polymer rich region could be under mechanical stress, which could lead to cracks in the film. This is not observed in our system, which, in the limit of no solvent, is well above the glass transition.

The magnitude of the density gradient depends on time and has a counter-effect of becoming a barrier to solvent evaporation, which in turn results in a solvent density gradient within the system as shown in figure 2(b). As a result, the concentration of solvent monomers remaining in the film [19] is found to be exponentially decreasing with time, in agreement with the experimental observations of Richardson *et al* [31]. The film thickness is also found to decrease exponentially with time.

The evaporation of solvent from multi-block copolymer films displays similar behaviour as that of homopolymers. Results for systems II and IV during the evaporation process are shown in figure 1. The two important evaporation features, polymer density gradient at the interface and a decrease in film thickness to reach its equilibrium density, observed in homopolymers are also observed for all of the multi-block copolymer systems studied. Previously, we [14] found that at least for ordered system I, differences in stiffness between the block segments influence the evaporation process considerably. Though the solvent is neutral, its transport property in the systems is found to depend on the relative stiffness between the two blocks. For blocks with the same stiffness, the solvent is equally distributed between the two blocks, while diffusion of solvent is observed exclusively through the softer segments as the relative stiffness between the two increases. However, in order to screen the unfavorable interaction between the two blocks, the solvent also tends to collect in the interfacial region as can be seen in figure 1. As a result, the rate of solvent evaporation, the width of the polymer/vapour interface, and the final morphologies of the films depend on the stiffness of the block segments. For the various block stiffnesses studied, the same exponential solvent evaporation behaviour is observed, but the rate of evaporation is found to decrease as the stiffness of the block segments increases. The interface width, on the other hand, is found to depend on the relative stiffness of the polymer segments. At the end of evaporation, for system I with $k_{\theta,2} = 3$, the morphology is found to be mainly lamellar, while an ordered microphase separated phase with cylindrical features is formed for $k_{\theta,2} = 1$.

The final morphologies of the polymer films depend on a number of factors, though here we focus on the effect of the block length. In reality, synthesizing perfectly ordered multiblock copolymers is difficult and, therefore, to mimic reality in the simulation the block lengths of the systems studied are chosen randomly from the values given in table 1. The dependence of morphology on block length can be seen from figures 3 and 4 where the resulting morphologies after evaporation for two ranges of block lengths are shown. As seen in figure 4 the flexible part of the segment is mainly exposed to the surface since it has a lower surface tension. As expected, the width and the spacing between the two domains increases with increasing block length. For systems II–IV the softer part of the segment percolates while the stiffer one does not.

4. Interdiffusion

4.1. Interdiffusion of solvent into a homopolymer film

Consider an equilibrated polymer film placed in contact with a thick layer of solvent. With time the solvent diffuses into the polymer film. In figure 5(a) the density profile of both polymer and solvent is shown as a function of time for a polymer film which is far above its glass transition temperature. The polymer relaxes as the solvent diffuses into polymer film from the right

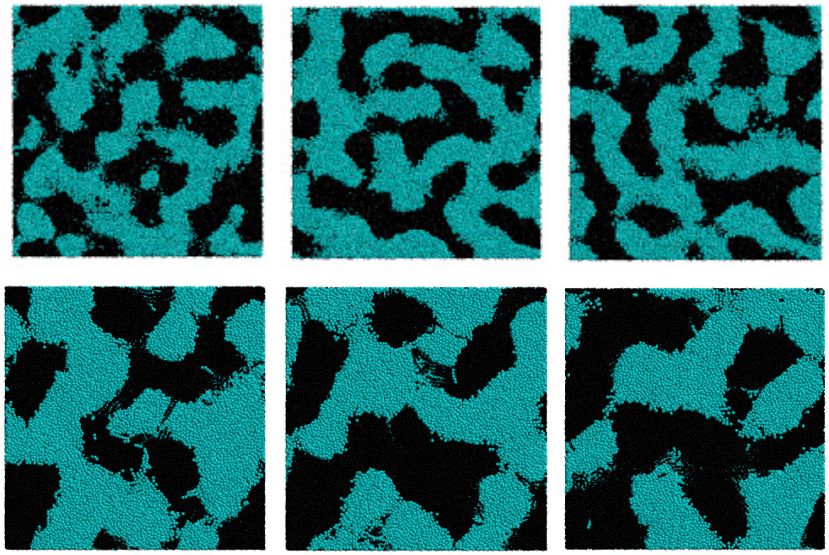

Figure 3. After evaporation of solvent, slices showing the top view of system II (top row) and system IV (bottom row) at heights of 15σ, 20σ, and 25σ, respectively, from the substrate. The thickness of the films is about 40σ.

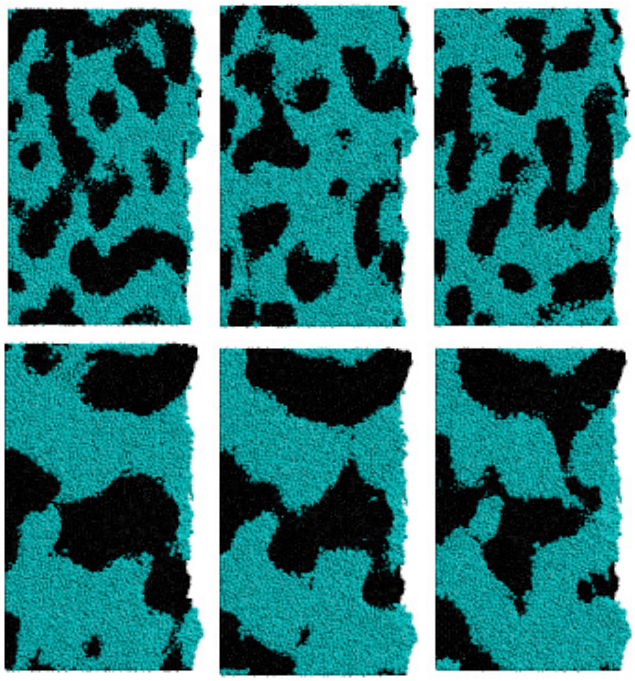

Figure 4. Vertical morphology cuts of the yz plane at $x = 25\sigma, 30\sigma$, and 35σ for system II (top row) and system IV (bottom row). Note that the right end of the slices is part of the surface of the film.

side, smearing out the boundary. The density profiles at different times have the same shape, differing slightly only in timescale. The position of the interface is found to increase with

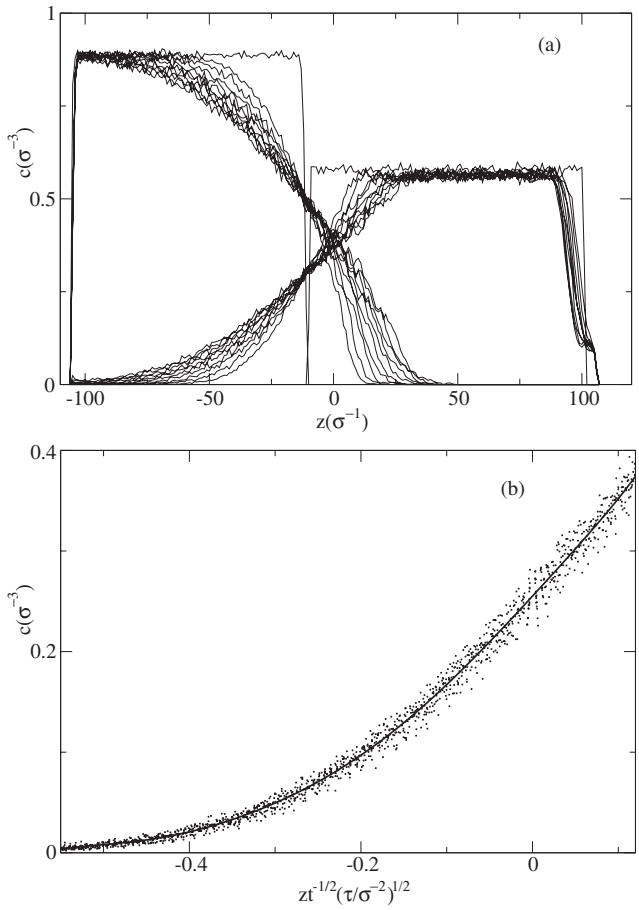

Figure 5. (a) Polymer and solvent concentration profiles as a function of time starting from $t = 0$ and plotted every 2400τ and (b) solvent concentration profiles replotted as a function of the scaling variable $zt^{-1/2}$. The solid line in (b) represents the theoretical curve based on equation (2).

$t^{1/2}$ in agreement with Fickian diffusion behaviour. This can be further seen by re-plotting the solvent density profile of figure 5(a) as a function of $\eta = z/t^{1/2}$ as shown in figure 5(b). As expected for Fickian diffusion behaviour, the profiles collapse on to a single master curve. In addition, equation (3) can be integrated to yield the diffusivity at concentration c'

$$D(c') = -\frac{1}{2}\left[\left(\frac{\mathrm{d}c}{\mathrm{d}\eta}\right)\right]_{c'}^{-1} \int_0^{c'} \eta \,\mathrm{d}c \tag{7}$$

where $\eta = z/t^{1/2}$. Thus from the scaled concentration profile one can directly obtain the diffusivity $D(c)$.

Applying equation (7) to the master curve of the solvent concentration profile, $c(\eta)$, the diffusivity of the solvent as a function of solvent concentration can be determined. First $c(\eta)$ was fitted to a polynomial function of at least order five, i.e. to obtain an optimal fit to the data, and then $c(\eta)$ is integrated analytically to the target concentration using the transformation $\int_0^{c'} \eta \,\mathrm{d}c = \int_{\eta_0}^{\eta} \eta \frac{\mathrm{d}c}{\mathrm{d}\eta} \mathrm{d}\eta$. The diffusivity $D(c)$ calculated by repeating this procedure for different values of solvent concentration is shown in figure 6 (closed circles). The diffusivity is

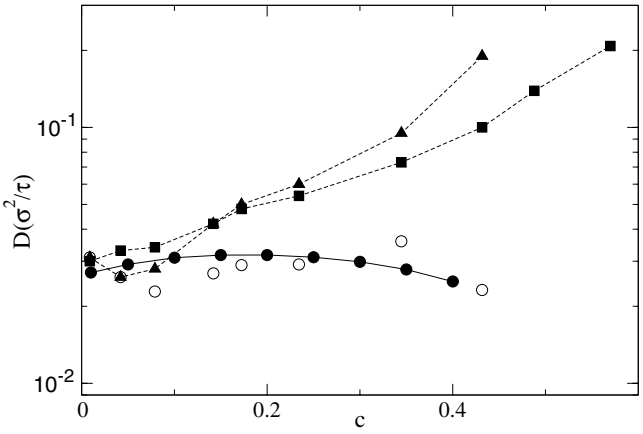

Figure 6. Dependence of diffusion constants on solvent concentration for $D_s(c)$ (■) and $D_c(c)$ (▲); closed circles are for $D(c)$ determined from the concentration profile using equation (2) while open circles are for $D(c)$ determined from the Darken equation (8). The lines are a guide to the eye.

approximately a constant within the error of the simulation, $D(c) \simeq 0.033 \pm 0.004\sigma^2/\tau$. This constant value for $D(c)$ in turn was used in equation (2) and the calculated concentration profile is shown in figure 5(b) as solid lines. In the region of interest, the calculated concentration profile fits reasonably well to the simulated concentration profile.

A number of relations between $D(c)$ and equilibrium diffusion constants have been proposed. The most common is the Darken equation [33–35]

$$D(c) = D_c(c)\left(\frac{\partial \ln f}{\partial \ln c}\right)_T \tag{8}$$

where $D_c(c)$ is the corrected diffusivity and is related to molecular mobility and f is the fugacity of the solvent in the polymer. Equation (8) assumes that diffusion is driven by gradients in chemical potential. The corrected diffusion coefficient $D_c(c)$ of the solvent in the polymer can be calculated using the Einstein form equation

$$D_c(c) = N_T x_s x_p \lim_{t\to\infty} \frac{1}{6t}\langle\{[\mathbf{r}_{cm,s}(t) - \mathbf{r}_{cm,s}(0)] - [\mathbf{r}_{cm,p}(t) - \mathbf{r}_{cm,p}(0)]\}^2\rangle \tag{9}$$

where x_i and $\mathbf{r}_{cm,i}(t)$ are the mole fraction and centre of mass of all monomers of species i at time t, and $N_T = N_s + N_p$ is the total number of monomers. Note that $D_c(c)$ is equal to the self-diffusion constant $D_s(c)$ of the solvent only in the limit $c \to 0$.

The fugacity f can be determined by applying the particle insertion method [27] and using the grand canonical MD code LADERA [36]. During the course of an equilibrium MD simulation, the energy E of inserting a solvent particle at random locations is sampled. The excess chemical potential energy μ_e is computed using

$$\mu_e = -k_B T \ln\langle\exp(-E/k_B T)\rangle. \tag{10}$$

The activity coefficient, γ, is then computed via $\gamma = \exp(\mu_e/k_B T)$. The thermodynamic factor in equation (8) can be expressed in terms of the activity coefficient γ of the solvent as

$$\frac{\partial \ln f}{\partial \ln c} = 1 + \frac{\partial \ln \gamma}{\partial \ln c}. \tag{11}$$

In the limit of low solvent concentration, $D(c) \simeq D_c(c)$ since the thermodynamic factor goes to unity.

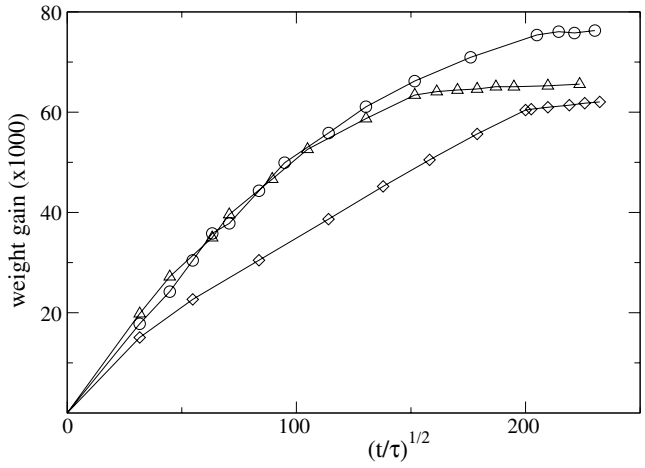

Figure 7. Weight gain in terms of the number of solvent monomers diffused into the polymer at a given time t for system II (□), system III (○), and system IV (△).

The diffusivity $D(c)$ determined from the Darken equation (equation (8)) is compared to that determined directly from the interdiffusion simulations in figure 6 as a function of concentration. Also shown are the self-diffusion, $D_s(c)$, and the corrected diffusion constant, $D_c(c)$. These diffusion constants show an exponential dependence on solvent concentration. However, the fugacity of the solvent was found to decrease monotonically with concentration [28]. This may sound counterintuitive, but since the solvent swells the polymer it is easier to insert solvent monomer as the density of solvent increases. Apart from the scatter in the data due to uncertainty in determining the thermodynamic factor, the diffusivity calculated from the two different approaches shows good agreement. At low solvent concentration $D(0) \approx D_c(0) = D_s(0)$, as expected.

Finally, we would like to point out that while the diffusivity shown in figure 6 is nearly independent of concentration this is not normally the case. In general $D(c)$ depends strongly on the state of the polymer as we have shown recently [29]. Only far above the glass transition temperature of the homopolymer is $D(c)$ constant. At lower temperatures, $D(c)$ becomes concentration dependent as the effective temperature of the polymer melt is reduced towards its glass transition temperature. The behaviour of $D(c)$ and the form of the concentration profile were also found to be related. The shape of the solvent concentration profile is changed from concave to convex as $D(c)$ is changed from being a constant to concentration dependent.

4.2. Interdiffusion of solvent into a block copolymer film

Diffusion of solvent into multiblock copolymers strongly depends on the orientation of microdomains to the film surface. Solvent diffusion coefficients were found to be higher for microdomains oriented perpendicular to the film surface than for microdomains oriented parallel to the surface. As shown in figure 1 the microdomain orientation for the systems used for the interdiffusion study is on average normal to the interface.

The rate at which the solvent penetrates into the polymer can be determined either taking the location of the polymer–solvent interface or the weight gain by the polymer as a function of time. Figure 7 shows the amount of solvent absorbed by the copolymer films versus $t^{1/2}$. Since the film surfaces after evaporation are somewhat rough, the solvent layer was placed just above

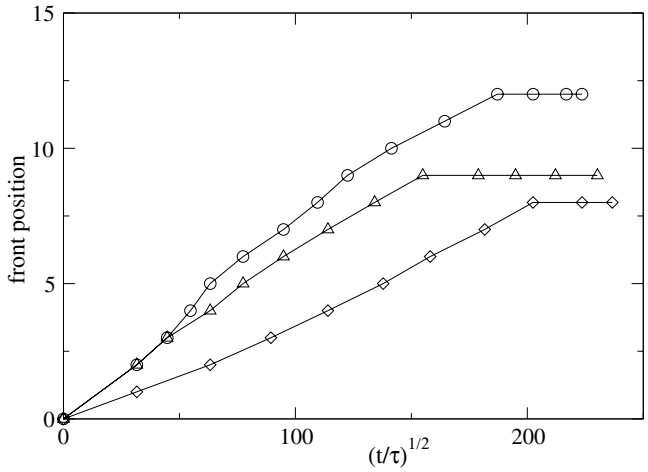

Figure 8. The location of the polymer segment–solvent interface as a function of time for system II (□), system III (○), and system IV (△).

the highest point of the polymer film. As a result, the very early time data for the interdiffusion are somewhat ill defined. However, after a short time the solvent fills in the gap between the film and the initial solvent layer. For all the systems, figure 7 shows approximately linear dependence on $t^{1/2}$ up to the saturation point. This indicates that the diffusion behaviour of the solvent in all the systems is Fickian. The rate of solvent absorption, the slope of the curve, of systems III and IV is the same, though system IV absorbs a smaller amount of solvent, which is comparable to that of system II, at saturation. Note that the surface area of the film is fixed and is only allowed to expand in the normal to the surface direction. This constraint may place limits on the extent of swelling and may have resulted in an earlier saturation of the systems than would have been observed experimentally.

To further investigate the diffusion behaviour of the solvent, the position of the polymer–solvent interface as a function of time is shown in figure 8. Since the flexible part of the segment has lower surface tension, the interface is basically between the flexible block part of the segment and the solvent. The position of the interface, shown in figure 8, on average shows a $t^{1/2}$ dependence in agreement with the homopolymer result and also the Fickian behaviour observed by figure 7. This is because the solvent swells the flexible block part of the chain and thus the diffusion of solvent mainly takes place through the flexible block segments.

It is important to consider the effect of block connectivity on the motion of the block segments of the copolymers. Since the blocks are covalently bonded, their dynamics is constrained as reflected in the dependence of the interface position of the copolymers on the length of the blocks. For system II, which has shorter block segments, the motions of flexible and stiff block segments are highly correlated. That is, in order to swell the flexible segment normal to the surface the stiff segment has to be stretched. However, for system III and IV the flexible part can swell significantly without stretching the stiff block segment.

5. Conclusion

Large scale molecular dynamics and grand canonical Monte Carlo simulation techniques were used to study solvent evaporation from homopolymer and heteropolymer films along with the interdiffusion of solvent into this films. As in most cases, where the structure of the film is

not know *a priori*, the model polymer films were produced by dissolving the polymer in a solvent and subsequently evaporating the solvent. This method produces structures that are in local equilibrium as in experiments. As the solvent evaporates, a sharp increase in the polymer density at the film/vapour interface is observed which creates a polymer density gradient that acts as a barrier for further solvent evaporation. For both homopolymer and heteropolymer films, the rate of solvent evaporation was found to be an exponentially decreasing function of time. In addition, for multiblock copolymer films the rate of solvent evaporation, the width of the polymer/vapour interface, and the resulting domain structure were found to be dependent on the stiffness of the block segments. We also showed that the final morphologies of the multiblock films strongly depend on the block length.

The reverse process, that is the interdiffusion of solvent into a polymer film, was also studied. For homopolymer films the weight gain by the polymer matrix increased as $t^{1/2}$ in agreement with Fickian diffusion. The diffusivity $D(c)$ as a function of concentration was determined from the solvent concentration profile using the one-dimensional Fick's diffusion equation. The dependence of the diffusivity $D(c)$ on solvent concentration was found to be strongly dependent on the state of the polymer. The diffusivity is approximately a constant for a polymer far above its glass transition temperature, but then becomes concentration dependent as one approaches the glass transition temperature. The behaviour of $D(c)$ and the shape of the solvent concentration profile was found to be directly related. The diffusivity calculated from the solvent concentration profile is in good agreement with the diffusivity calculated from an equilibrated solvent-polymer mixture using the Darken equation.

For multiblock copolymer films, where the stiffer block is below its glass transition temperature, the solvent swelled the softer block of the segment. In this case, the weight gain by the polymer matrix was found to be in accordance with Fickian diffusion.

Acknowledgment

Sandia is a multiprogramme laboratory operated by Sandia Corporation, a Lockheed Martin company, for the United States Department of Energy's National Nuclear Security Administration under contract No DE-AC04-94AL85000.

References

[1] Sonnenburg J, Gao J and Weiner J H 1990 *Macromolecules* **23** 4653
[2] Müller-Plathe F 1996 *Chem. Phys. Lett.* **252** 419
[3] Charati S G and Stern S A 1998 *Macromolecules* **31** 5529
[4] van der Vegt N F A 2000 *Macromolecules* **33** 3153
[5] Yi X and Pellegrino J 2002 *J. Polym. Sci.* B **40** 980
[6] Lim S Y, Tsotsis T T and Sahimi M 2003 *J. Chem. Phys.* **119** 496
[7] Crank J 1975 *The Mathematics of Diffusion* (Oxford: Oxford University Press)
[8] Csernica J, Baddour R F and Cohen R E 1987 *Macromolecules* **20** 2468
[9] Lin H, Steyerl A, Satija S K, Karim A and Russell T P 1995 *Macromolecules* **28** 1470
[10] Zielinski J M, Heuberger G, Sillescu H, Wiesner U, Heuer A, Zhang Y and Spiess H W 1995 *Macromolecules* **28** 8287
[11] Horstmann M, Urbani M and Veeman W S 2003 *Macromolecules* **36** 6797
[12] Lodge T P, Hamersky M W, Hanley K J and Huang C 1997 *Macromolecules* **30** 6139
[13] Miller-Chou B A and Koenig J L 2003 *Macromolecules* **36** 4851
[14] Tsige M, Mattsson T R and Grest G S 2004 *Macromolecules* **37** 9132
[15] Polson J M and Zuckermann M J 2000 *J. Chem. Phys.* **113** 1283
[16] Cooke I R and Williams D R M 2004 *Macromolecules* **37** 5778
[17] Auhl R, Everaers R, Grest G S, Kremer K and Plimpton S J 2003 *J. Chem. Phys.* **119** 12718

[18] Murat M, Grest G S and Kremer K 1999 *Macromolecules* **32** 595
[19] Tsige M and Grest G S 2004 *Macromolecules* **37** 4333
[20] Grest G S and Kremer K 1986 *Phys. Rev.* A **33** 3628
[21] Kremer K and Grest G S 1990 *J. Chem. Phys.* **92** 5057
[22] Baljon A R C and Robbins M O 2001 *Macromolecules* **34** 4200
[23] Sides S W, Grest G S and Stevens M J 2002 *Macromolecules* **35** 566
[24] Sides S W, Grest G S and Lacasse M D 1999 *Phys. Rev.* E **60** 6708
[25] Thompson A P and Heffelfinger G S 1999 *J. Chem. Phys.* **110** 10693
[26] Plimpton S J 1995 *J. Comput. Phys.* **117** 1
[27] Heffelfinger G S and Ford D M 1998 *Mol. Phys.* **94** 659
[28] Tsige M and Grest G S 2004 *J. Chem. Phys.* **120** 2989
[29] Tsige M and Grest G S 2004 *J. Chem. Phys.* **121** 7513
[30] Bornside D E, Macosko C W and Scriven L E 1989 *J. Appl. Phys.* **66** 5135
[31] Richardson H, Carelli C, Keddie J L and Sferrazza M 2003 *Eur. Phys. J.* E **12** e2004
[32] de Gennes P G 2002 *Eur. Phys. J.* E **7** 31
[33] Darken L S 1948 *Trans. AIME* **175** 184
[34] Maginn E J, Bell A T and Theodorou D N 1993 *J. Phys. Chem.* **97** 4173
[35] Skoulidas A I and Sholl D S 2001 *J. Phys. Chem.* B **105** 3151
[36] Thompson A P and Heffelfinger G S 1999 *J. Chem. Phys.* **110** 10693